Supporting Material: Platelet Transport Rates and Binding Kinetics at High Shear over a Thrombus

David L. Bark, Jr.[1] and David N. Ku[1]

[1] **Georgia Institute of Technology, GWW School of Mechanical Engineering, Atlanta, GA, United States**

Supporting Material: Methods

Field Potential for Mass Transport

The field potential is used to create a forcing function that drives platelets away from a high hematocrit, represented by:

Equation S1

$$\nabla \psi_{RBC} = \nabla(c_{RBC}), \qquad \nabla \psi_{platelet} = \nabla(\phi c_{platelet})$$

RBCs use a typical field potential, corresponding to Fick's law. However, the platelet field potential is defined as a function of hematocrit. Platelets are assumed to respond passively to RBCs without influence on the RBC motion. Platelets are assumed to move down a RBC gradient, but as a function of the platelet number, providing the first half of:

Equation S2

$$\nabla \psi_{platelet} = c_{platelet} \nabla(\phi) + \phi \nabla(c_{platelet})$$

Platelets also move down their own concentration gradient, defined as the second half of Eq. S2. The potential in the second half is a function of hematocrit due to the likelihood for a collision with another cell. These terms are distinct from enhanced diffusivity because enhanced diffusivity defines the rate at which transport occurs, as opposed to the direction. However, the field potential drives the platelets in a specific direction that should be a function of the colloidal components in the flow. As both gradients reach equilibrium or as one particle concentration becomes 0, the transport across streamlines goes toward 0. In this regard, when hematocrit is 0, platelets are dependent on thermal diffusivity, which is negligible in comparison to situations where RBCs are present. Therefore, Eq. 1 was chosen as the simplest form of a field potential that incorporates platelets and RBCs into the model based on the requirements for platelet motion in a

directed path. The sensitivity for this choice can be determined by comparing case ii and case iii in Figure 3.

Concentration Profiles Applied at Inlet and Drift Term for Platelets and RBCs

A concentration profile for red blood cells (RBCs) is required for the drift term used in the model and is also used as an inlet profile condition for RBCs. We assumed a blunt RBC concentration profile to best match the profile shown in Aarts et al. (26). The profile was created by assuming that the profile followed a hyperbolic tangent, which is the same form as a profile presented by Hund and Antaki (35):

Equation S3

$$c_{RBC} = \lambda_1 \left(1 + \tanh\left[\beta(r/R - \delta)\right]\right)$$

where while β and δ are used to shape the profile. Values for these constants are determined by a curve fit to Aarts et al. (26). These constants are sufficient for the drift function. However, the constant, λ_1, is also required to define the concentration profile supplied as an inlet boundary condition for RBCs. The value for λ_1 can be estimated by equating the average hematocrit with the area-average of Eq. S1 across a straight vessel with the radius, R. Upon integration, λ_1 is substituted into Eq. S1, resulting in:

Equation S4

$$c_{RBC,eq} = \frac{\overline{c}_{RBC} R^2 \left(1 + \tanh\left[\beta(r/R - \delta)\right]\right)}{2\int_0^R r\left(1 + \tanh\left[\beta(r/R - \delta)\right]\right)dr}$$

where $\overline{c}_{RBC}$ is the area-averaged RBC concentration across the vessel at the inlet.

For the initial concentration profile of platelets, the profile was determined under the assumption that the flux across the vessel radius is equal to zero. The profile of

platelets is controlled by the field potential, Eq. 4, resulting in an inverse relationship between the RBC and platelet profile, which is related by a constant, λ_2:

Equation S5

$$C_{platelet} = \frac{\lambda_2}{C_{RBC}}$$

The constant for the platelet concentration profile can then be estimated based on the known inlet average concentration of platelets and a known RBC concentration profile:

Equation S6

$$C_{platelet} = \frac{R^2 \overline{C}_{platelet}}{(C_{RBC})2\int_0^R \frac{rdr}{(C_{RBC})}}$$

$$= \frac{4\beta^2 \overline{C}_{platelet}}{(1+\tanh[\beta(r/R-\delta)])[2\beta^2 - e^{2\beta(\delta-1)}(2\beta - e^{2\beta} + 1)]}$$

where $\overline{C}_{platelet}$ is the area-averaged platelet concentration at the inlet.

Deriving the Leveque Model for a Cylindrical Vessel

The convection-diffusion equation is simplified to develop an expression for platelet deposition rates based on transport for estimating the rate of thrombus growth. The model consists of flow through an axisymmetric straight cylindrical vessel. We simplify the convection-diffusion mass transport equation by eliminating the unsteady term, since thrombus grows at a maximum of approximately 2 platelets/μm^2-min and platelets enter a coronary artery at a rate that is an order of magnitude higher, 64 platelet/μm^2-min ($J_{in}=Q\overline{C}_{platelet}/A$). The calculation assumes the flow rate, Q, is 2 ml/s, the bulk concentration of platelets, $\overline{C}_{platelet}$, is 225,000 platelets/μl, and a vessel diameter of 3 mm. Flow is assumed to be fully developed. Axial convection is assumed to

dominate over axial diffusion. Additionally, the field potential is assumed to be equal to the platelet concentration. Therefore, the convective-diffusion equation simplifies to:

Equation S7

$$v_x \frac{\partial c_{platelet}}{\partial x} = D_{platelet} \left(\frac{1}{r} \frac{\partial}{\partial r} \left(\frac{\partial c_{platelet}}{\partial r} \right) \right)$$

where v_x is the axial velocity, r is the radial coordinate, and x is the axial coordinate. Near the wall, we approximate the velocity as $\dot{\gamma}_w y$, where y is the normal distance from the wall and $\dot{\gamma}_w$ is the wall shear rate, commonly known as the Lévêque approximation. This near-wall approximation assumes a linear velocity gradient. Coordinates are converted to a distance from the wall, y, which is assumed to be much smaller than the radius. To solve for the new equation we can use a similarity variable (1):

Equation S8

$$\eta = \left(\frac{\dot{\gamma}_w}{D_{platelet} x} \right)^{1/3} y$$

We solve for concentration with respect to the similarity variable:

Equation S9

$$c_{platelet} = A \int_0^{\eta} e^{-\frac{1}{9}\eta^3} d\eta + B$$

where A and B are integration constants. We now require boundary conditions for mass transport. We use Dirichlet and Neumann boundary conditions to solve Eq. S7:

Equation S10

$$c_{platelet} \big|_{\eta \to \infty} = \bar{c}_{platelet}$$

$$J_{\eta \to 0} = D_{platelet} \frac{\partial c_{platelet}}{\partial \eta} \frac{\partial \eta}{\partial y} \bigg|_{\eta \to 0} = k_t c_{platelet} \big|_{\eta \to 0}$$

where k_t is the kinetic binding rate constant of a platelet to the thrombus site. The resulting flux of platelets predicted to arrive at the surface is:

Equation S11

$$J_{platelet} = \frac{\bar{c}_{platelet}}{\dfrac{1}{k_t} + \dfrac{1.86}{\left(\dfrac{\dot{\gamma} D_{platelet}^2}{x} \right)^{1/3}}}$$

The axial dimension, x, is set at *3R*, corresponding to the stenosis apex. The chosen axial dimension also assumes that thrombus only forms over the stenosis region. *3R* was chosen because the stenosis apex is where most thrombus occurred experimentally.

Computational Implementation

Computations were performed on a Dell 64 bit precision T7400 with two quad-core Intel Xeon x5472@3.00 GHz processors with 2.99 GHz, 16.0 GB of RAM. Simulations were performed in series, despite the multi-core processors. Simulations were typically run at 0.1 s per iteration with 60 spatial iterations per time step. It took approximately 2 days to run a simulation that results in thrombus growth to occlusion.

Peclet Number at Stenosis Apex

The Peclet number is defined by a ratio of advection to diffusion. It is of interest for evaluating the importance of margination in transport phenomena in the vicinity of a stenosis. A high Peclet number means that diffusion is much slower than advection, which affects the platelet distribution after a flow disturbance. The Peclet number is calculated by:

6

Equation S12

$$Pe = \frac{LU}{D}$$

where L is the characteristic length, U is the average velocity, and D is the diffusivity coefficient. We use the characteristic length of the vessel radius at the stenosis apex. Also, the diffusivity coefficient is estimated by enhanced diffusivity:

Equation S13

$$D = ka^2 c_{RBC}(1 - c_{RBC})^n \dot{\gamma} + D_{th}$$

where k is a constant at 0.15, a is a scale for particle collisions and is taken as the approximate radius of a RBC, 4 μm, ϕ is the local hematocrit, n is a constant at 0.8 ± 0.3, and $\dot{\gamma}$ is the local shear rate (24). Thermal motion is neglected since it is much slower than shear dependent enhanced diffusivity. Furthermore, if we assume a parabolic velocity profile, we can relate the shear rate to the average velocity:

Equation S14

$$\dot{\gamma} = 4U / R$$

Therefore, the Peclet number ($c_{RBC} = 45\%$) can be represented as as:

$$Pe = \frac{RU}{ka^2 c_{RBC}(1 - c_{RBC})^n 4U / R} = \frac{R^2}{2.7 \times 10^{-6} \text{ mm}^2}$$

Vessels ranging from a radius of 0.075 mm for a severely stenotic vessel to 3 mm for an open coronary artery result in a Peclet number ranging from 10^4 to 10^6. The high Peclet number illustrates that diffusion is relatively slow compared to advection and therefore, the flow disturbances from a stenosis should disturb margination.

Results

Equilibrium Concentration Profiles

RBCs localize to the center of cylindrical vessels, while platelets marginate to the outer edge of vessels. To verify that the model exhibits this behavior, we compared the model to experimental data of Aarts et al. (26), who evaluated platelet and RBC concentration profiles in a 3 mm vessel. Profiles predicted by the model matched well with that of Aarts et al. for 20% hematocrit, Figure S1. While, the RBC profile was determined by a curve fit, Eq. 7/S2, the platelet concentration profile is based on our field potential term, Eq. 4, which did not involve a curve fit. Values were further determined for a 40% hematocrit. The RBC profile was determined based on a curve fit of Eq. 7/S2 to the data of Aarts et al. The platelet profiles for a hematocrit of 40% matched well with the literature (26, 36, 46), as depicted in Figure S2. Note that these results are extended to a hematocrit of 45% in the manuscript because an average of 45% was found over multiple samples in porcine blood used in the experiments (38). Computed profiles scale with the vessel radius.
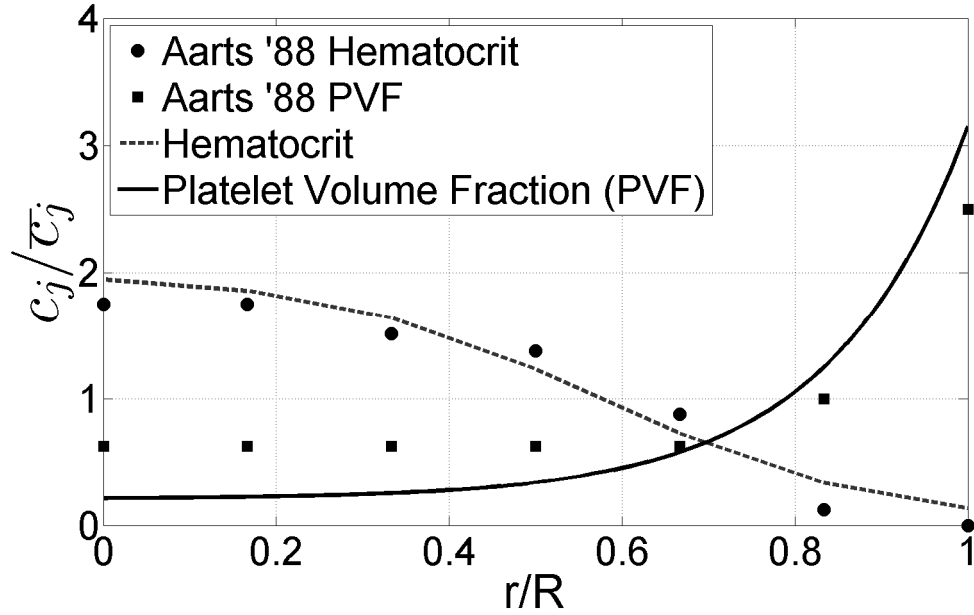
Figure S1: A plot of computed platelet volume fractions from the model based on a hematocrit profile that was determined from a curve fit to the data in Aarts et al. (26) for an overall hematocrit of 0.2. The computed platelet volume fraction is plotted relative to measured platelet volume fractions by Aarts et al.
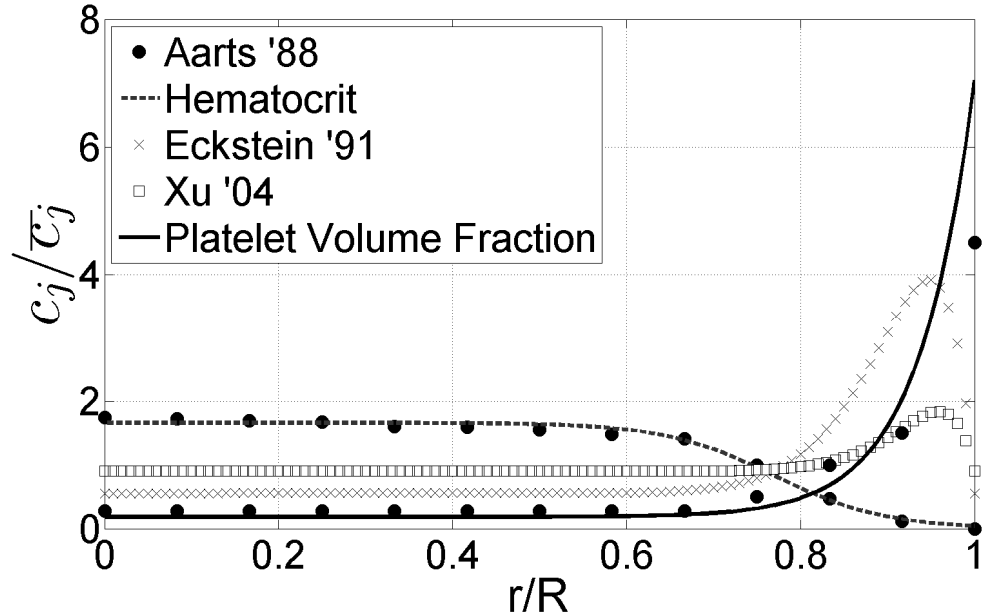

Figure S2: Distribution of RBCs and platelets with margination. The graph shows our modeled platelet volume fraction and hematocrit as a function of radial position in comparison with three references. The equilibrium profile was set to match an example RBC profile from the Aarts et al. (26). The resulting peak of the platelet concentration profile matches well with the literature (26, 36, 46)

1.   Lévêque, A. 1928. Les Lois de la transmission de chaleur par convection, par
        André Lévêque. Dunod.